EPJ Web of Conferences **42**, 02005 (2013)
DOI: 10.1051/epjconf/20134202005

A dispersive optical model potential for nucleon induced reactions on ^{238}U and ^{232}Th nuclei with full coupling

José Manuel Quesada[1,a], Efrem S. Soukhovitskii[2], Roberto Capote[3], and Satoshi Chiba[4]

[1] Departamento de Física Atómica, Molecular y Nuclear, Universidad de Sevilla , Apartado 1065, 41080, Sevilla, España
[2] Joint Institute for Energy and Nuclear Research 220109, Minsk-Sosny, Belarus
[3] NAPC–Nuclear Data Section, International Atomic Energy Agency, Vienna International Centre, A–1400, Vienna, Austria
[4] Research Laboratory for Nuclear Reactors, Tokyo Institute of Technology 2-12-1-N1-9 Ookayama, Meguro-ku, Tokyo 152–8550, Japan

Abstract. A dispersive coupled-channel optical model potential (DCCOMP) that couples the ground-state rotational and low-lying vibrational bands of ^{238}U and ^{232}Th nuclei is studied. The derived DCCOMP couples almost all excited levels below 1 MeV of excitation energy of the corresponding even-even actinides. The ground state, octupole, beta, gamma, and non-axial bands are coupled. The first two isobar analogue states (IAS) populated in the quasi-elastic (p,n) reaction are also coupled in the proton induced calculation, making the potential approximately Lane consistent. The coupled-channel potential is based on a soft-rotor description of the target nucleus structure, where dynamic vibrations are considered as perturbations of the rigid rotor underlying structure. Matrix elements required to use the proposed structure model in Tamura coupled-channel scheme are derived. Calculated ratio $R(U238/Th232)$ of the total cross-section difference to the averaged σ_T for ^{238}U and ^{232}Th nuclei is shown to be in excellent agreement with measured data.

1 Introduction

High accuracy requirements were placed on inelastic cross-sections of reactions induced by neutrons on the major component of nuclear reactor fuel ^{238}U in the whole energy range up to 20 MeV by the OECD/NEA WPEC SG-26 [1]. The improvement of cross sections and emission spectra and reduction of their uncertainties for neutron induced reactions on ^{238}U is an important issue that should initiate new theoretical studies. It is well known that the optical model is one of the fundamental theoretical tools forming the basis of nuclear reaction modelling. Using the optical model one can calculate not only total, elastic and reaction cross sections, but also transmission coefficients for the statistical and pre-equilibrium model calculations. Thus, a phenomenological optical model potential that is capable of describing with high accuracy available scattering data over a wide energy range is essential to meet data needs mentioned above.

2 Dispersive coupled-channel optical model potential with full coupling

Nucleon-nucleus optical model calculations are a solution of the quantum-mechanics scattering problem. Improvement of optical model predictions implies addressing the following three areas of work:

[a] e-mail: quesada@us.es

– Further development of the coupled-channel optical model for actinides (e.g. achieving a Lane consistent model).
– Usage of better nuclear structure models providing realistic scattering dynamics and a proper description of complex low-lying structure of actinide nuclei.
– Development of accurate and fast computational algorithms (considering that the expanded coupling scheme, which now couples many more levels than in the standard approach, significantly increases computational time of the optical model parameters fitting to available experimental data and requires higher numerical accuracy).

A detailed formulation of the dispersive coupled-channel optical model potential was given in previous works [2–4]; a brief summary is given in the next Section. We focus in this contribution on the second area of development, namely on improving the model of nuclear structure used in coupled-channel calculations. The third goal implied to implement our main computational tool - the OPTMAN code [5,6] - in a 64-bit platform, also introducing the use of quadruple precision (REAL*16) in critical areas of the code to ensure computational stability with the extended coupling scheme. Description of these changes are outside the scope of present contribution and will be presented elsewhere.

2.1 The dispersive nature of DCCOMP

In a dispersion relation treatment, the real potential strength consists of a term which varies slowly with energy, the so called Hartree-Fock (HF) term, $V_{HF}(\mathbf{r}, E)$, plus a correction (dynamical or polrization) term, $\triangle V(\mathbf{r}, E)$, which is calculated using a dispersion relation. Under favorable conditions of analyticity in the complex E-plane the real part ΔV can be constructed from the knowledge of the imaginary part W on the real axis through the dispersion relation

$$\Delta V(\mathbf{r}, E) = \frac{\mathcal{P}}{\pi} \int_{-\infty}^{\infty} \frac{W(\mathbf{r}, E)}{E - E} dE \,, \tag{1}$$

where we have now explicitly indicated the radial and energy dependence of these quantities and $\mathcal{P}$ means that the principal value of the integral should be taken. To simplify the problem, the geometry of the imaginary terms of the DCCOMP are usually assumed to be energy-independent and they are expressed in terms of a Woods-Saxon function $f_{WS}(r, R_i(\theta, \varphi))$ or $g_{WS}(r, R_i(\theta, \varphi))$ - it's derivative. In such case the radial functions factorize out of the integrals and the energy-dependence is completely accounted for by two overall multiplicative strengths $\Delta V(E)$ and $W(E)$. Both of these factors contain, we note, volume and surface contributions. A similar assumption is used for the spin-orbit potential where the real spin-orbit strength consists of a term which varies slowly with energy $V_{SO}(\mathbf{r}, E)$, plus a correction term, $\triangle V_{SO}(\mathbf{r}, E)$, which is calculated using a dispersion relation (1).

2.2 Lane consistency of the DCCOMP and excitations of the Isobaric Analog States (IAS)

Our previously developed isospin-dependent DCCOMP for actinides [3,4] has been shown [7] to be approximately Lane consistent, and described the direct quasi-elastic (p,n) scattering to the IAS of the target nucleus. The corresponding coupling form-factors for the charge-exchange calculations using the dispersive coupled-channel potential were defined in Ref.[7]. These couplings allowed the use of available IAS scattering data (angular distributions) during the fitting procedure of the optical potential parameters. IAS data proved critical to consistently estimate the strength of the isovector component. However, we should mention that there are still open questions on how to deal with Coulomb corrections to the imaginary potential, and how to achieve the consistency of corresponding dispersive contributions. Those problems will be addressed in a future paper.

2.3 Nuclear Shapes and coupling potential multipoles for even-even nuclei

The traditional soft-rotator model [9,10] considers nuclei to be dynamically deformable around the equilibrium spherical shape. Both axial and non-axial vibrations are possible; the low-lying states

of even-even nuclei can be considered as a combination of rotation, β-quadrupole, η-octupole, γ-quadrupole and higher order axial vibrations ($\lambda = 4, 6, 8$). Namely, the soft-rotator model assumes that instant nuclear shapes of even-even nucleus can be described as:

$$R(\theta,\varphi) = R_0 \left\{ 1 + \beta_2 \left[\cos\gamma Y_{20}(\theta) + \frac{1}{\sqrt{2}} \sin\gamma \left[Y_{22}(\theta,\varphi) + Y_{2-2}(\theta,\varphi) \right] \right] \right. \quad (2)$$
$$\left. + \beta_3 \left[\cos\eta Y_{30}(\theta) + \frac{1}{\sqrt{2}} \sin\eta \left[Y_{32}(\theta,\varphi) + Y_{3-2}(\theta,\varphi) \right] \right] + \sum_{\lambda=4,6,8} \beta_{\lambda 0} Y_{\lambda 0}(\theta) \right\}$$

The soft rotator model of nuclear structure has been successfully applied in coupled-channels optical model analyses for many nuclei starting from ^{12}C [11, 12]. However, so far we have been unable to derive a dispersive coupled channel optical model potential for actinides. Dispersive optical model features a reduced number of parameters compared to traditional OMP analyses, therefore parameter compensation of model defects become more difficult.

We traced our problem in fitting actinide data to the occurrence of big static deformations in actinide nuclei at low excitation energies. Such deformations are not dynamical as required for the soft-rotator model, but stable static deformations. Indeed, it is well known that a rigid rotor model very well characterizes properties of even-even actinides. Many optical model potentials for actinides have relied on this fact to describe nucleon scattering on these nuclei; in particular a DCCOMP had been successfully derived [2–4].

However, needed higher accuracy of data for fast neutron reactors requires improving the description of scattering data at energies from 100 keV up to 2–3 MeV. While the nuclear structure of even-even actinides below 500 keV corresponds to a rigid rotor, above 500 keV several vibrational bands are observed in the excited spectrum that are much better described by the soft rotor. This fact has long been recognized, a vibrational-rotational description within the coupled-channel approach have been used to describe data by several authors[13–16]. We propose a new solution to the problem derived from the soft-rotator description of the low-lying nuclear structure of actinides, but consistent with the rigid-rotor behaviour at low excitation energies.

Mathematically, the failure of the traditional soft-rotator model applied to actinides is due to the very slow convergence of the multipolar expansion of the soft-rotor potential around spherical shape for stable deformed shapes. To solve this problem we consider that the quadrupole dynamical variable β_2 of the soft rotor model contains a big static axial component β_{20} plus a small dynamical contribution $\delta\beta_2$. Additionally, we assume that a dynamical variable γ is small. With these assumptions we can rewrite eq.(2) as:

$$R(\theta,\varphi) = R_0 \left\{ 1 + \sum_{\lambda=2,4,6,8} \beta_{\lambda 0} Y_{\lambda 0}(\theta) + \left[\delta\beta_2 - \gamma\beta_{20} \frac{\gamma}{2} \right] Y_{20}(\theta) + \gamma\beta_{20} \frac{1}{\sqrt{2}} \times \right. \quad (3)$$
$$\left. \left[Y_{22}(\theta,\varphi) + Y_{2-2}(\theta,\varphi) \right] + \beta_3 \left[\cos\eta Y_{30}(\theta) + \frac{1}{\sqrt{2}} \sin\eta \left[Y_{32}(\theta,\varphi) + Y_{3-2}(\theta,\varphi) \right] \right] \right\} + o(\gamma^3, \gamma\delta\beta_2)$$

where the term $R_0 \left[1 + \sum_\lambda \beta_{\lambda 0} Y_{\lambda 0}(\theta,\varphi) \right]$ in eq.(3) corresponds to the axially-symmetric equilibrium shape (rigid rotor). The small departures from rigid-rotor shape are considered up to second order in quadrupole non-axiality parameter γ and to all orders in octupole non-axiality parameter η. Therefore the calculations have been performed within the rigid rotor model with soft-rotator corrections. The observed low-lying collective levels of even-even actinides are described by adjusting the Hamiltonian parameters in the soft-rotator nuclear model [9, 10]; soft-rotator deformation parameters β_2, β_3, γ and η are derived from the fitting of structure data.

If we further assume that the octupole dynamical deformation parameters β_3 and η are small, we can expand the nuclear potential as done by Tamura (see eq.(5) of ref.[17]) to get:

$$V(r,\theta,\varphi) = \left[V(r,\theta,\varphi) \right]_{(\delta\beta_2=0,\gamma\beta_{20}=0,\beta_3=0)} + \left[\frac{\partial}{\partial R} V(r,\theta,\varphi) \right]_{(\delta\beta_2=0,\gamma\beta_{20}=0,\beta_3=0)} \times \quad (4)$$
$$\left\{ \left[\delta\beta_2 - \gamma\beta_{20} \frac{\gamma}{2} \right] Y_{20}(\theta) + \gamma\beta_{20} \frac{1}{\sqrt{2}} \left[Y_{22}(\theta,\varphi) + Y_{2-2}(\theta,\varphi) \right] + \beta_3 \left[\cos\eta Y_{30}(\theta) + \frac{1}{\sqrt{2}} \sin\eta \left[Y_{32}(\theta,\varphi) + Y_{3-2}(\theta,\varphi) \right] \right] \right\}$$

Then we perform the multipole expansion of $V_i(r,\theta,\varphi)$ in terms of the spherical harmonics :

$$V_i(r,\theta,\varphi) = \sum_{\lambda\mu} v^{(i)}_{\lambda\mu}(r) Y_{\lambda\mu}(\theta,\varphi) \tag{5}$$

where

$$V_1(r,\theta) = \left[V(r,\theta,\varphi)\right]_{(\delta\beta_2=0,\gamma\beta_{20}=0,\beta_3=0)} \;\; ; \;\; V_2(r,\theta) = \left[\frac{\partial}{\partial R} V(r,\theta,\varphi)\right]_{(\delta\beta_2=0,\gamma\beta_{20}=0,\beta_3=0)} \tag{6}$$

Knowing the nuclear structure and corresponding nuclear shape, we can calculate the coupled-channel matrix elements needed in reaction calculations, where effective values of the dynamic deformations (formally averaged over intrinsic states) are multiplied by the relevant reduced matrix elements. Using Tamura's notations ([17, 18]), the matrix element couplings can be expressed as:

$$\begin{aligned}
< i|V(r,\theta,\varphi)|f > = & \sum_{\lambda\ even} v^{(1)}_{\lambda}(r) < IK||D^{\lambda}_{;0}||I'K' > \\
& + \frac{\left[\delta\beta_2 - \gamma\beta_{20}\frac{\gamma}{2}\right]_{eff}}{2} \sum_{\lambda\ even} \left[\tilde{v}^{(2)}_{\lambda}(r)\right]_0 < IK||D^{\lambda}_{;0}||I'K' > \\
& + \frac{[\gamma\,\beta_{20}]_{eff}}{\sqrt{2}} \sum_{\lambda\ even} \left[\tilde{v}^{(2)}_{\lambda}(r)\right]_2 < IK|| \left(D^{\lambda}_{;2} + D^{\lambda}_{;-2}\right) ||I'K' > A(lI;l'I';\lambda J) \\
& + [\beta_3\ \cos\eta]_{eff} \sum_{\lambda\ odd} \left[\tilde{v}^{(3)}_{\lambda}(r)\right]_0 < IK||D^{\lambda}_{;0}||I'K' > \\
& + \frac{[\beta_3\ \sin\eta]_{eff}}{\sqrt{2}} \sum_{\lambda\ odd} \left[\tilde{v}^{(3)}_{\lambda}(r)\right]_2 < IK|| \left(D^{\lambda}_{;2} + D^{\lambda}_{;-2}\right) ||I'K' > A(lI;l'I';\lambda J)
\end{aligned} \tag{7}$$

with $A(lI;l'I';\lambda J)$ given by:

$$A(lI,l'I';\lambda J) = \frac{1}{4\pi}(-1)^{J-I'+l+l'+\frac{1}{2}(l'-l)} \hat{l}\hat{l}' < ll'00|\lambda 0 > W(lIl'I';J\lambda) \tag{8}$$

and :

$$\begin{aligned}
v^{(i)}_{\lambda}(r) &= 2\pi \int_{-1}^{1} d(cos(\theta))\ V_i(r,\theta) \\
\left[\tilde{v}^{(2)}_{\lambda}(r)\right]_0 &= \sum_{\lambda'\ even} v^{(2)}_{\lambda'}(r) \left[\frac{5(2\lambda'+1)}{4\pi(2\lambda+1)}\right]^{1/2} < \lambda' 200|\lambda 0 >^2 \\
\left[\tilde{v}^{(2)}_{\lambda}(r)\right]_2 &= \sum_{\lambda'\ even} v^{(2)}_{\lambda'}(r) \left[\frac{5(2\lambda'+1)}{4\pi(2\lambda+1)}\right]^{1/2} < \lambda' 200|\lambda 0 >< \lambda' 202|\lambda 2 > \\
\left[\tilde{v}^{(3)}_{\lambda}(r)\right]_0 &= \sum_{\lambda'\ even} v^{(2)}_{\lambda'}(r) \left[\frac{7(2\lambda'+1)}{4\pi(2\lambda+1)}\right]^{1/2} < \lambda' 300|\lambda 0 >^2 \\
\left[\tilde{v}^{(3)}_{\lambda}(r)\right]_2 &= \sum_{\lambda'\ even} v^{(2)}_{\lambda'}(r) \left[\frac{7(2\lambda'+1)}{4\pi(2\lambda+1)}\right]^{1/2} < \lambda' 300|\lambda 0 >< \lambda' 302|\lambda 2 >
\end{aligned} \tag{9}$$

The relevant reduced matrix elements are calculated as follows

$$\begin{aligned}
< I0||D^{\lambda}_{;0}||I'0 > &= \sqrt{2I'+1} < I'\lambda 00|I0 > \ \text{for}\ K=0 \\
< IK||D^{\lambda}_{;0}||I'K' > &= \delta_{K,K'} \sqrt{2I'+1} \frac{[1+(-1)^{\lambda}]}{2} < I'\lambda K0|IK > \ \text{for}\ K \neq 0 \\
< I0||(D^{\lambda}_{;2} + D^{\lambda}_{;-2})||I'K' > &= \sqrt{2I'+1} \times \frac{[1+(-1)^{\lambda-I}]}{\sqrt{2}} < I'\lambda K' - 2|I0 >
\end{aligned} \tag{10}$$

3 Results and conclusions

A new DCCOMP with energy independent geometry has been derived for nucleon scattering on ^{238}U and ^{232}Th nuclei with the following properties:

- It is based on dispersive relations and Tamura coupled-channel formalism.
- DCCOMP parameters were fitted to reproduce the whole database of neutron and proton scattering data including low-energy observables (e.g. neutron strength functions) and the quasielastic (p,n) angular distributions (IAS excitation).
- Coupled-channels calculations are based on rigid rotor model with soft rotator corrections (almost all discrete levels below 1 MeV in excitation energy have been considered, including the ground state band coupled to vibrational octupole, beta, gamma and non-axial bands as well as 2 isobar analog states for the (p,n) channel).

Energy-averaged total cross sections σ_T for ^{238}U and ^{232}Th nuclei from 5 to 200 MeV, which were measured by Abfalterer et al.[20] were used to calculate the experimental cross-section ratio $R(238U/232Th)$ and associated uncertainty. This *figure of merit* is known to be very sensitive to the quality of the optical model potential. Calculated results are compared with data [20] in Fig.1. The DCCOMP parameterization derived in this work is in excellent agreement with Abfalterer measurements. Reasonable agreement is also shown by previous dispersive coupled-channel potential (RIPL-2408) [3,4,19], as well as for the Lane-consistent semi-microscopic folding model of Bauge et al.[22]. Conventional nondispersive coupled-channel potentials fail to reproduce the experimental data as can be seen for the RIPL 2601 potential [19,21].

Further work is ongoing to guarantee the full Lane consistency of the potential and to derive the final parameter set.

References

1. M. Salvatores (*coord.*), OECD/NEA WPEC Subgroup 26 Final Report *Uncertainty and Target Accuracy Assessment for Innovative Systems Using Recent Covariance Data Evaluations*, NEA Tech. Rep. No. **6410** (2008)
2. E.Sh. Soukhovitskiĭ, R. Capote, J.M. Quesada and S. Chiba, Phys. Rev. **C72** (2005) 024604.
3. R. Capote, E.Sh. Soukhovitskiĭ, J.M. Quesada and S. Chiba, Phys. Rev. **C72** (2005) 064610.
4. R. Capote, S. Chiba, E.Sh. Soukhovitskiĭ, J.M. Quesada, and E. Bauge, J. Nucl. Sci. Technol. **45** (2008) 333.
5. E.Sh. Soukhovitskiĭ, G.B. Morogovskiĭ, S. Chiba, O. Iwamoto, and T. Fukahori, *Physics and Numerical Methods of OPTMAN: A Coupled-channels Method Based on Soft-rotator Model for a Description of Collective Nuclear Structure and Excitation*. JAERI Tech. Rep. **JAERI-Data/Code 2004-002**, Japan (2004).
6. E.Sh. Soukhovitskiĭ, S. Chiba, R. Capote, J.M. Quesada, S. Kunieda and G.B. Morogovskiĭ, JAERI Tech. Rep. **JAERI-Data/Code 2008-025**, Japan (2008).
7. J.M. Quesada, R. Capote, E.Sh. Soukhovitskiĭ, S. Chiba, Phys. Rev. **C76** (2007) 057602.
8. A.M. Lane, Phys. Rev. Lett. **8** (1962) 171 .
9. Y.V. Porodzinskiĭ, E.Sh. Sukhovitskiĭ, Sov. J. Nucl. Phys. **54** (1991) 570.
10. Y.V. Porodzinskiĭ, E.Sh. Sukhovitskiĭ, Phys. Atom. Nucl. **59** (1996) 228 .
11. E.Sh. Sukhovitskiĭ, S. Chiba, O. Iwamoto, and Y.V. Porodzinskiĭ, Nucl. Phys. **A640** 147–162 (1998).
12. J.-Y.Lee, E.Sh. Soukhovitskiĭ, Y. Kim, R. Capote, S. Chiba, and J.M. Quesada, J. Kor. Phys. Soc. **59**, 1019–1022 (2011).
13. D.W. Chan et al, Phys. Rev. **C26** (1982) 841.
14. D.W. Chan et al, Phys. Rev. **C26** (1982) 861.
15. E. Sheldon. L.E. Beghian, D.W. Chan et al, J.Phys.G:Nucl. Phys. **12** (1986) 443.
16. T. Kawano, N. Fujikawa and Y. Kanda, Technical Report **INDC(JPN)-169** (1993).
17. T. Tamura, Rev. Mod. Phys. **17** (1965) 679–708.

18. T. Tamura, Nucl. Phys. **A73** (1965) 241.
19. R. Capote, M. Herman, P. Oblozinsky, et al., Nucl. Data Sheets **110** (2009) 3107 (Available from *http://www-nds.iaea.org/RIPL-3/*).
20. W.P. Abfalterer, F.B. Bateman, F.S. Dietrich, R.W. Finlay, R.C. Haight, and G.L. Morgan, Phys. Rev. **C63** (2001) 044608.
21. E.Sh. Soukhovitskiĭ, S. Chiba, J.-Y. Lee, O. Iwamoto, T. Fukahori, J. Phys.G: Nucl. Part. Phys.**30** (2004) 905.
22. E. Bauge, J.P. Delaroche, and M. Girod, Phys. Rev., **C63** (2001) 024607.

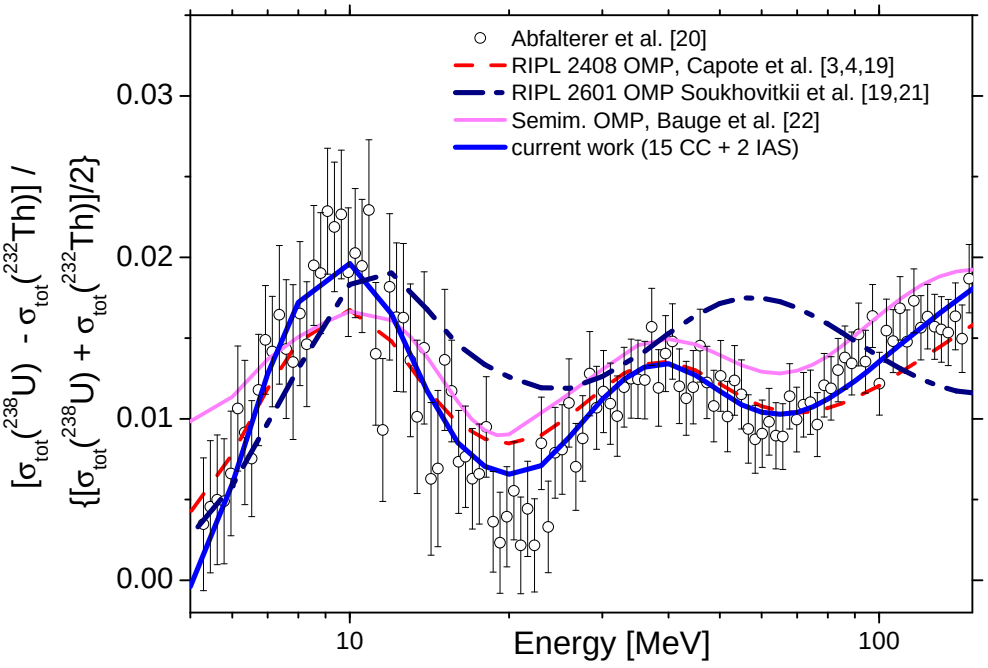

Fig. 1. Figure of merit: energy dependence of measured total cross section ratio [σ_{tot}(^{238}U)- σ_{tot}(^{232}Th)] /{[σ_{tot}(^{238}U)+ σ_{tot}(^{232}Th)]/2}